J Mater Sci (2008) 43:3604–3607
DOI 10.1007/s10853-008-2571-8

Is ferroelectricity in $BiMnO_3$ induced by superlattice?

H. Yang · Z. H. Chi · J. L. Jiang · W. J. Feng · J. F. Dai · C. Q. Jin · R. C. Yu

Received: 11 February 2008 / Accepted: 21 February 2008 / Published online: 23 March 2008

Abstract The room-temperature structures of the $BiMnO_3$ ceramic sample synthesized under high pressure have been investigated using transmission-electron microscopy (TEM) and theoretical simulations. The electron diffraction (ED) data revealed that the stoichiometric $BiMnO_3$ crystallizes in the centrosymmetric $C2/c$ structure, and not in the noncentrosymmetric $C2$ structure. This was confirmed by further calculations of high-resolution transmission-electron microscopy (HRTEM) images. A second polymorph, characterized as a body-centered pseudocubic superstructure with the lattice constants of $4a_p \times 4b_p \times 4c_p$, was also found in the present sample. Composition analyses and image simulations revealed that this superlattice was formed as the result of an ordered oxygen deficiency. In terms of crystallography, we suggest that the weak ferroelectric polarizations measured on the $BiMnO_3$ samples originate from the superlattice. This work is very important for further studies of $BiMnO_3$ and structurally related compounds.

H. Yang (✉)
State Key Laboratory of Gansu Advanced Non-ferrous Metal Materials, Lanzhou University of Technology, Lanzhou 730050, P.R. China
e-mail: hyang@lut.cn

H. Yang · J. L. Jiang · W. J. Feng · J. F. Dai
School of Science, Lanzhou University of Technology, Lanzhou 730050, P.R. China

Z. H. Chi · C. Q. Jin · R. C. Yu
Laboratory for Extreme Condition Physics, Beijing National Laboratory for Condensed Matter Physics, Institute of Physics, P.O. Box 603, Beijing 100080, P.R. China

R. C. Yu
e-mail: rcyu@aphy.iphy.ac.cn

Introduction

$BiMnO_3$ with a highly distorted perovskite-type structure has been extensively studied as a multiferroic material. Among ABO_3-type multiferroic oxides, $BiMnO_3$ is a unique compound that displays true ferromagnetic behaviors with a Curie temperature (T_C) of $\sim$105 K [1–6]. $BiMnO_3$ is also expected to be ferroelectric according to the first-principle calculations [7, 8]. However, ferroelectricity is difficult to observe due to the low resistance of films and the lack of large high-quality bulk samples. Experimentally dielectric hysteresis loops have been measured on only few samples of $BiMnO_3$ [9, 10], and the measured ferroelectric polarization [9, 10] is much smaller than the result calculated from first principle [11], making it difficult to associate the measured hysteresis loops to bulk ferroelectricity.

Ferroelectricity requires that the crystal structure be noncentrosymmetric and the ferroelectric transition is directly related to the structural phase transformation. At room temperature, $BiMnO_3$ has a highly distorted perovskite-type structure, and was primitively reported to be of a triclinic lattice with $a = c \approx 3.935$ Å, $b \approx 3.989$ Å, $\alpha = \gamma \approx 91.47°$, and $\beta \approx 91.97°$ [12]. Later, an ED observation by Chiba et al. [13] suggested a 4-fold periodicity along the $[111]_p$ direction (where the subscript 'p' refers to the fundamental perovskite-type cell). Based on the electron diffraction information, the crystal structure of $BiMnO_3$ was refined from powder neutron diffraction data to be a $C2$ monoclinic structure with $a = 9.53$ Å, $b = 5.61$ Å, $c = 9.85$ Å, and $\beta = 110.67°$ [14]. This structure was commonly accepted and used as a fundamental model for interpretation of the observed physical phenomena. However, very recently Belik et al. [6] observed the [010] zone-axis ED pattern of $BiMnO_3$ in

which the $h0l$ reflections with $l = 2n + 1$ are absent (hereinafter the indices and zone axes without the subscript 'p' are given in the monoclinic supercell), and suggested that this extinction is due to the existence of the c-glide plane perpendicular to the b^*-axis. The space group of $BiMnO_3$ was therefore determined to be $C2/c$ based on the transmission-electron microscopy (TEM) observation, and the structural data were also refined from neutron powder diffraction [6]. Thus two space groups, $C2$ and $C2/c$, were assigned to $BiMnO_3$, and the former one is noncentrosymmetric while the latter one is centrosymmetric. In terms of crystallography, the noncentrosymmetric $C2$ structure is expected to be ferroelectric. Furthermore, a room-temperature polymorph, i.e., the $4a_p \times 4b_p \times 4c_p$ superlattice, was also reported in $BiMnO_3$ [5, 13, 15]. To further study the ferroelectricity in $BiMnO_3$, it is very important to clarify its room-temperature structures.

Below room temperature, the monoclinic structure of $BiMnO_3$ appears to be stable [3, 16]. Two high-temperature structure changes have been reported to occur at 450 and 770 K [2–4, 17]. The phase transformation at 450 K is monoclinic-to-monoclinic without any detectable change in the symmetry [3, 17]. The phase transformation at 770 K is monoclinic-to-orthorhombic [3, 17]. The origin of both the high-temperature phase transitions has not been determined yet. In this paper, we mainly focus on the investigation of the room-temperature structures of $BiMnO_3$ using TEM and theoretical simulations and try to discuss the origin of the ferroelectricity in $BiMnO_3$.

Experimental

Polycrystalline $BiMnO_3$ ceramic was prepared by a high-pressure synthesis method described in Ref. [4]. A stoichiometric mixture of Bi_2O_3 (Alfa Aesar 99.99%) and Mn_2O_3 (Alfa Aesar 98%) was ground thoroughly in an agate mortar followed by calcination in alumina crucible at 600 K for 24 h, and then subjected to high-pressure synthesis (5 GPa and 1,173 °C for 30 min) using a cubic-anvil-type apparatus. Thin foils for TEM studies were prepared by crushing $BiMnO_3$ ceramic in an agate mortar filled with alcohol and then dispersing the fine fragments suspended in alcohol on a microgrid. A Tecnai F20 field-emission transmission-electron microscope was used for ED and HRTEM experiments. All the TEM studies were carried out at an acceleration voltage of 200 keV.

Results and discussion

The important differences in electron diffraction between the proposed $C2$ and $C2/c$ structures of $BiMnO_3$ [6, 14] would be shown on the [010] zone axis. To see which one of the two structural models is valid, it is extremely important to investigate the [010] ED pattern. As there are a number of very similar ED patterns in $BiMnO_3$, we conducted systemic tilting experiments to assign the correct zone axis. Figure 1 shows the ED pattern taken along the [010] zone-axis direction. It is obvious that the $00l$ reflections with $l = 2n + 1$ are absent on this zone axis as indicated by arrows. This extinction condition is attributed to the existence of the c-glide plane perpendicular to the b^*-axis. In addition, very weak $h0l$ reflections are seen to appear for $h = 2n + 1$ (one of the reflections is marked by the white open circle). The appearance of those weak reflections is likely due to the double diffraction. The resultant ED data clearly suggest that $BiMnO_3$ crystallizes in the $C2/c$ structure [6], not in the $C2$ structure [14].

To further confirm that $BiMnO_3$ indeed forms the $C2/c$ structure, we also carried out the HRTEM studies. The most informative images are obtained along the [110] zone axis. Figure 2a shows an HRTEM image taken along this zone axis. This image was obtained from a thin region of the crystal under the defocus value of ~ -70 nm. Figure 2b shows a theoretical image, calculated from the $C2/c$ structural model [6], as a function of thickness (from 3.3 to 17.7 nm) for a defocus value of -70 nm. It is clear that the calculated image fits perfectly with the experimental confirming the $C2/c$ structural model.

A second room-temperature polymorph, the $4a_p \times 4b_p \times 4c_p$ superlattice, was revealed by TEM observation to commonly exist in the high-pressure $BiMnO_3$ samples

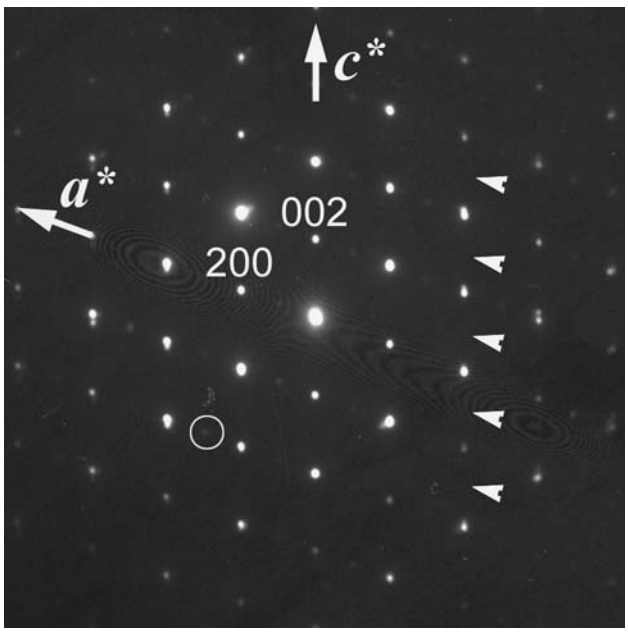

Fig. 1 ED pattern of $BiMnO_3$ taken along the [010] zone-axis direction, showing that the $00l$ reflections with $l = 2n + 1$ are absent on this zone axis as indicated by arrows

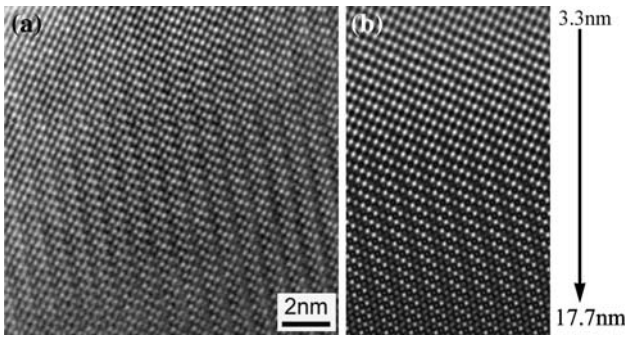

Fig. 2 (**a**) Experimental HRTEM image of $BiMnO_3$ taken along the [110] zone axis. (**b**) A theoretical image, calculated from the *C*2/*c* structural model [6], as a function of thickness for a defocus value of −70 nm. It is clear that the calculated image fits perfectly with the experimental confirming the *C*2/*c* structural model

[5, 13]. This superstructure was also observed in our $BiMnO_3$ sample. Figure 3a and b displays the $[010]_p$ and $[111]_p$ zone-axis ED patterns of the superstructure, respectively. Based on the ED patterns, this form can be characterized as a body-centered pseudocubic superstructure with the lattice constants of $4a_p \times 4b_p \times 4c_p$. During our TEM observation, we found that the superstructure can develop from the C2/*c* form under strong electron beam irradiation.

To see whether chemical effects result in the $4a_p \times 4b_p \times 4c_p$ superlattice, electron energy-loss spectroscopy (EELS) and energy dispersive X-ray (EDX) techniques were combinatively used to analyze its composition. The results showed that the analyzed composition slightly deviates from the stoichiometric $BiMnO_3$ with about two oxygens missing from one $4a_p \times 4b_p \times 4c_p$ supercell. This indicates that the formation of the superlattice is ascribed to an ordered oxygen deficiency. To further confirm the origin of the superlattice, the HRTEM images were simulated from an idealized structure model with the assumption that one supercell contains just two oxygen vacancies. A simulated image along the $[111]_p$ zone axis is embedded on the experimental one and presented in Fig. 4. It is clear that the simulated image fits perfectly with the experimental, confirming that the superlattice indeed originates from the ordered oxygen deficiencies.

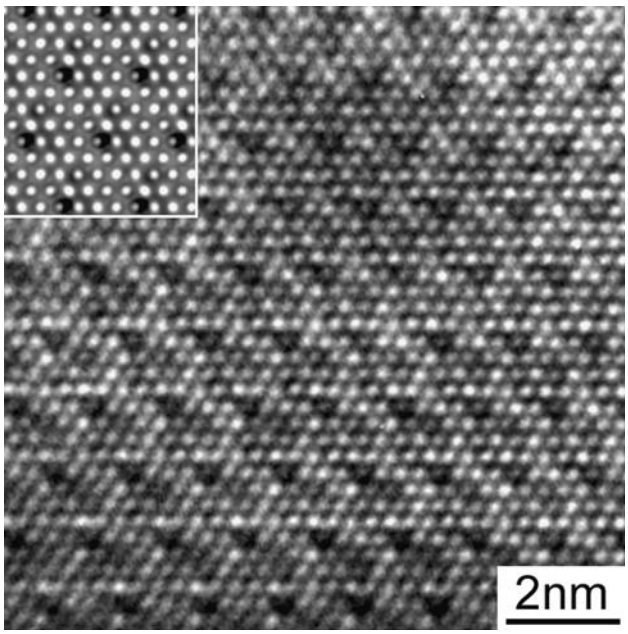

Fig. 4 $[111]_p$ HRTEM image of the superlattice taken under the defocus value of approximately −55 nm. A simulated image (thickness: 31.5 nm, defocus value: −55 nm), calculated from an idealized structure model with the assumption that one supercell contains just two oxygen vacancies, is superimposed onto the experimental to produce the good agreement

Our experimental and theoretical studies demonstrate that at room temperature the stoichiometric $BiMnO_3$ crystallizes in the centrosymmetric *C*2/*c* structure, but not in the noncentrosymmetric *C*2 structure. Note that the first-principle calculations on $BiMnO_3$ also showed that the *C*2/*c* structure with zero polarization is more stable than the

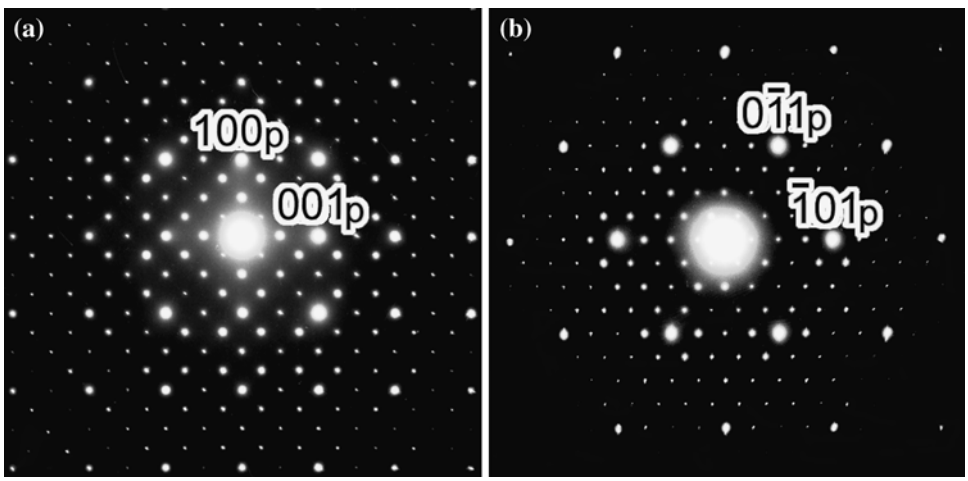

Fig. 3 ED patterns of the $4a_p \times 4b_p \times 4c_p$ superlattice taken along (**a**) $[010]_p$ and (**b**) $[111]_p$ zone axes. The indices and zone axes are given in the fundamental perovskite subcell

$C2$ structure at 0 K [18]. In terms of crystallography, the centrosymmetric $C2/c$ structure, reported to be stable below 450 K [3, 16], is not expected to be ferroelectric. Maybe this is why the bulk ferroelectricity is difficult to observe in $BiMnO_3$. The weak ferroelectric polarizations measured on the rare examples of $BiMnO_3$ samples [3, 9, 10] possibly originate from other mechanisms, such as an electronic phase transition triggered by an electric field, and the local structural distortion from centrosymmetric to noncentrosymmetric caused by the tiny changes of the stoichiometry [6]. The $4a_p \times 4b_p \times 4c_p$ superstructure, revealed to be formed as the result of an ordered oxygen deficiency, can be considered as the potential candidate for the appearance of ferroelectricity.

Recently, a large number of researches have shown that ferroelectrics can be synthesized by the superlattice approach. A typical example is where ferroelectricity has been induced in the artificial $SrTiO_3/SrZrO_3$ superlattice fabricated by molecular beam epitaxy [19], although neither $SrTiO_3$ nor $SrZrO_3$ is ferroelectric. The superlattice-induced ferroelectricity is commonly explained as the result of the lattice distortion. Lattice distortion is also induced in the ordered oxygen-deficient superlattice of $BiMnO_3$. Since two adjacent Mn atoms are always separated by an oxygen atom in the stoichiometric $BiMnO_3$ structure, the removal of oxygen will inevitably result in a repulsion of the two positive Mn ions, consequentially leading to the lattice distortion from centrosymmetric to noncentrosymmetric. The noncentrosymmetric lattice distortion is expected to lead to the formation of spontaneous polarization in the superlattice.

In most cases, the oxygen-deficient superlattice was formed as a minor second phase in the $BiMnO_3$ samples. The formation of the superlattice can be reasonably understood since any factor that induces oxygen deficiency, such as the inhomogeneity of chemical composition, could result in the superlattice. Generally, it is not easy to control the superlattice during the sample preparation, and a tiny change of the experimental conditions (e.g., pressures, temperatures, sizes of the sample chamber, and the increase and decrease rates of temperature and pressure, etc.) could result in a different result to form the superlattice. The superlattice was also found to be able to develop from the $C2/c$ structure under strong electron beam irradiation. Preparation of single-phase superlattice sample of $BiMnO_3$ to further study its structures and properties would be very important to make the utilization of this oxide in potential applications.

Conclusions

TEM and theoretical simulations have been used to characterize the structures of the high-pressure synthesized perovskite-type $BiMnO_3$. The experimental and theoretical data revealed that the stoichiometric $BiMnO_3$ forms the centrosymmetric $C2/c$ structure instead of the noncentrosymmetric $C2$ structure. The $4a_p \times 4b_p \times 4c_p$ superlattice existing as a second polymorph in the sample was revealed by composition analyses and image simulations to be formed as the result of an ordered oxygen deficiency. The present work suggests that the weak ferroelectricity observed in the $BiMnO_3$ samples possibly originates from the oxygen-deficient superlattice.

Acknowledgements This work was supported by the Foundation of Gansu Educational Committee (0703B-01), the Science Foundation of Lanzhou University of Technology (SB10200701) and the Natural Science Foundation of Gansu Province (3ZS061-A25-039). R. C. Yu thanks the National Natural Science Foundation of China (Grant Nos. 10774168 and 50621061) and the State Key Development Program for Basic Research of China (Grant Nos. 2005CB623602 and 2007CB925003) for the support.

References

1. Sugawara F, Iida S, Syono Y, Akimoto S (1965) J Phys Soc Jpn 20:1529
2. Faqir H, Chiba H, Kikuchi M, Syono Y, Mansori M, Satre P, Sebaoun A (1999) J Solid State Chem 142:113
3. Kimura T, Kawamoto S, Yamada I, Azuma M, Takano M, Tokura Y (2003) Phys Rev B 67:180401(R)
4. Chi ZH, Xiao CJ, Feng SM, Li FY, Jin CQ, Wang XH, Chen RZ, Li LT (2005) J Appl Phys 98:103519
5. Montanari E, Righi L, Calestani G, Migliori A, Gilioli E, Bolzoni F (2005) Chem Mater 17:1765
6. Belik AA, Iikubo S, Yokosawa T, Kodama K, Igawa N, Shamoto S, Azuma M, Takano M, Kimoto K, Matsui Y, Takayama-Muromachi E (2007) J Am Chem Soc 129:971
7. Hill NA, Rabe KM (1999) Phys Rev B 59:8759
8. Seshadri R, Hill NA (2001) Chem Mater 13:2892
9. Moreira dos Santos A, Parashar S, Raju AR, Zhao YS, Cheetham AK, Rao CNR (2002) Solid State Commun 122:49
10. Chi ZH, Yang H, Feng SM, Li FY, Yu RC, Jin CQ (2007) J Magn Magn Mater 310:e358
11. Shishidou T, Mikamo N, Uratani Y, Ishii F, Oguchi T (2004) J Phys: Condens Matter 16:S5677
12. Sugawara F, Iiida S, Syono Y, Akimoto S (1968) J Phys Soc Jpn 25:1553
13. Chiba H, Atou T, Faqir H, Kikuchi M, Syono Y, Murakami Y, Shindo D (1998) Solid State Ionics 108:193
14. Atou T, Chiba H, Ohoyama K, Yamaguchi Y, Syono Y (1999) J Solid State Chem 145:639
15. Yang H, Chi ZH, Li FY, Jin CQ, Yu RC (2006) Phys Rev B 73:024114
16. Moreira dos Santos A, Cheetham AK, Atou T, Syono Y, Yamaguchi Y, Ohoyama K, Chiba H, Rao CNR (2002) Phys Rev B 66:064425
17. Montanari E, Calestani G, Migliori A, Dapiaggi M, Bolzoni F, Cabassi R, Gilioli E (2005) Chem Mater 17:6457
18. Shishidou T, Oguchi T (2006) Multiferroicity of BiMnO3 reexamined from first principles. Presented at APS March Meeting, Baltimore, MD
19. Tsurumi T, Harigai T, Tanaka D, Nam SM, Kakemoto H, Wada S, Saito K (2004) Appl Phys Lett 85:5016